Journal of Machine Engineering, 2026, Vol. 26
ISSN 1895-7595 (Print) ISSN 2391-8071 (Online)

Received*: 11 June 2025* / Accepted: *07 January 2026* / Published online: *24 January 2026*

machine metrology,
machine surface quality,
machining error detection

Vilhelm SÖDERBERG[1*], Robert TOMKOWSKI[1],
Toru KIZAKI[2], Yifu LIAO[2],
Andreas ARCHENTI[1]

IN SITU- ON MACHINE- POST PROCESS METROLOGY SYSTEM DESIGN FOR MACHINING SYSTEM CHARACTERIZATION

The evaluation of machine tool characteristics and their impact on surface quality is challenging, often requiring disruptive traditional methods. This study introduces a novel, non-invasive approach using optical camera images for rapid and accurate assessment. Data robustness was ensured by acquiring initial images outside the machining chamber with consistent external illumination, focusing on detailed intensity profile analysis. Machined surfaces were processed using intensity profile extraction and Fast Fourier Transform (FFT). The dominant spatial wavelength (0.1833 mm) consistently showed excellent agreement (within 1.85%) with the theoretical feed per revolution (0.1800 mm). This robustly validates the method's ability to precisely capture primary kinematic tool marks. Temporal information, inferred from spatial frequencies, underwent subsequent FFT to identify periodic phenomena and harmonics. The comprehensive spatial and temporal FFT analyses offer detailed, quantitative surface characterizations. The clear distinctions in temporal harmonic patterns provide robust, frequency-domain signatures informing machining system performance and process integrity.

1. INTRODUCTION

In cutting operations, the surface quality of a machined workpiece varies according to the extent to which the tool deviates from its commanded path. Such deviations stem from multiple factors, including the static and dynamic characteristics, thermal behaviour [1], and geometric accuracy of the machine tool's structure, as well as the drive system's properties such as servo synchronization accuracy and long-term effects like bearing wear. In other words, the final surface of the workpiece reflects the superimposed influences of these various characteristics.

Numerous methods have been proposed to measure and evaluate these factors individually. For instance, the Loaded Double Ball Bar (LDBB) method [2] can evaluate static

[1] Production Engineering, KTH Royal Institute of Technology, Sweden
[2] Mechanical Engineering, University of Tokyo, Japan
[*] E-mail: vilsod@ug.kth.se
https://doi.org/10.36897/jme/216462

characteristics that depend on direction, while techniques using vibrations arising during machining have been employed to assess dynamic characteristics [3]. Approaches that utilize many temperature sensors have also been reported for evaluating thermal deformation [4], [5]. Additionally, Double Ball Bar (DBB) is well known for measuring geometric error and servo synchronization accuracy [6, 7]. However, many of these methods often require interrupting the machining process, removing the workpiece for evaluation, or installing numerous sensors in advance. Such measurement tasks create downtime on the production line, compromising productivity.

To evaluate machine tool characteristics with high accuracy and in minimal time, Ibaraki and Okumura [8] proposed a method that leverages the machined workpiece itself. By measuring the machined surface with a touch-trigger probe, one can assess thermal errors. This technique is widely recognized and is included in Annex of ISO 10791-10 [9] for evaluating thermal deformation. Nonetheless, this approach only captures thermal deformation related errors, which represent just one factor among many that determine workpiece accuracy and surface quality.

Consequently, it remains challenging to quickly and accurately estimate all the machining process-related factors that influence the final quality of the work piece [10]. Still, because the final surface results from a superposition of all these characteristics, there is potential to conduct a comprehensive evaluation of the machine tool if the surface can be observed and measured by some means. Therefore, the present study aims to use a general-purpose camera, rather than a dedicated measurement device, to observe and measure the machined workpiece surface. In doing so, we seek to identify each characteristic of the machine tool in a short time while retaining high accuracy.

Several in-situ methods for observing machined surfaces using optical cameras have already been proposed. For example, Quinsat et al. [11] measured the surface of a workpiece mounted on a five-axis machining center using a sensor based on chromatic confocal sensing technology, integrated on the same machine. The papers [12 – 14], likewise report in-situ surface roughness measurement using chromatic confocal sensing technology. Although these techniques enable highly accurate measurement of surface roughness, they do not address the identification of other machine tool characteristics.

On the other hand, identifying each individual characteristic from the superimposed surface features is generally difficult. The static and dynamic characteristics, thermal properties, and geometric accuracy of the machine tool's structure, as well as drive system properties such as servo synchronization accuracy and the long-term effects of bearing wear, do not act independently but instead affect one another. For instance, changes in the temperature distribution can alter the pressure on contact interfaces, which in turn changes stiffness owing to nonlinear contact behaviour. Bearing wear could further influence static and dynamic characteristics as well as thermal behaviour. Under these complex interactions, constructing a geometry-based or physics-based model and then solving the inverse problem to isolate each factor proves difficult. Statistical methods particularly those incorporating machine learning are thus promising alternatives.

Machining is a forceful process that requires significant power, necessitating the encapsulation of the workpiece and tool within a machining chamber to protect the surrounding environment. The environment within the machining chamber is aggressive, characterized by vibrations, temperature fluctuations, and material removed from the workpiece. Additionally, fluids such as cutting fluids may be present, further contributing to harsh conditions. These aggressive conditions complicate the placement of analytical equipment within the machining chamber and impose additional requirements on processes to perform analyses, such as ensuring the cleanliness of the workpiece. However, the environment is not constant; it is most aggressive when the tool is engaged. The idea is to quickly collect necessary data during pauses in modern machining, such as tool or workpiece changes, to evaluate the process results with minimal impact on process time.

This study examines milling, which is characterized by a stationary workpiece and a moving tool. Material removal occurs intermittently, with the tool periodically engaging, leading to variations in forces. These variations must be mitigated to minimize their impact on the generated surface. The hypothesis is that images captured by a CCD camera of the machined surface contain sufficient data to detect specific frequencies, including vibrations. This research proposes a method for rapidly and accurately estimating machine tool characteristics. Specifically, by capturing images of the machined workpiece surface using an optical camera mounted on the machine tool. From multiple surface images, features such as the workpiece intensity profiles are extracted. Frequency analysis techniques are then employed to identify machining system and process characteristics. With this proposed method, the lengthy evaluations traditionally requiring specialized measurement devices can be performed more rapidly, without sacrificing accuracy.

2. MATERIALS AND METHODS

2.1. MACHINING

This research utilized a 3-axis vertical milling centre (Baca R1000) to perform dry machining on an aluminium Al6082. Several slots were milled using a 12 mm diameter, 2-flute solid end mill, with cutting parameters detailed in Table 1. Post-machining, the workpiece was inspected using a camera at 200x magnification. To ensure process stability, the initial 10 mm of each slot was excluded from data collection, and uniform illumination was maintained to guarantee data quality.

Table 1. Cutting parameters

Slots	Feed rate v_f [mm/min]	Feed per tooth [mm] $f_z = v_f/(n \cdot z)$	Spindle speed [rpm]	Depth of Cut [mm]
Odd (1, 3, 5, …)	540	0.09	3000	2
Even (2, 4, 6, …)	720		4000	

The number of flutes on a milling cutter is a critical parameter influencing performance primarily through its effect on chip load. Two-flute cutters, with their larger gullets, are effective for roughing softer materials like aluminium by efficiently evacuating large chips.

Conversely, multi-flute cutters are better for finishing harder materials, as their design produces a smoother surface finish and enhances tool rigidity, which minimizes chatter. While 2-flute tools allow for a heavier chip load per tooth, multi-flute tools can achieve higher material removal rates at increased rotational speeds and offer longer tool life by distributing wear.

2.2. IMAGE ACQUISITION AND ANALYSIS

In this study, a DinoLite AM7915MZT CCD camera was used. A protective enclosure has been designed for the camera to shield it from the machining environment. Special attention has been given to finding an appropriate placement for the camera.

Table 2. Specification of the CCD camera used for image acquisition

Manufacturer	Dino-lite
Model Number	AM7915MZT
Magnification	10x – 220x
Resolution	2592 × 1944

Collected images of machined surfaces are analysed in several steps, acquiring image, extraction of intensity profile, FFT analysis of spatial frequencies, converting spatial frequency to inferred temporal frequency (ITF), comparison of dominant spatial wavelength with theoretical feed per revolution, and finally calculating harmonics from ITF analysis. Schematic diagram of the image analysis is presented in the Fig. 1.

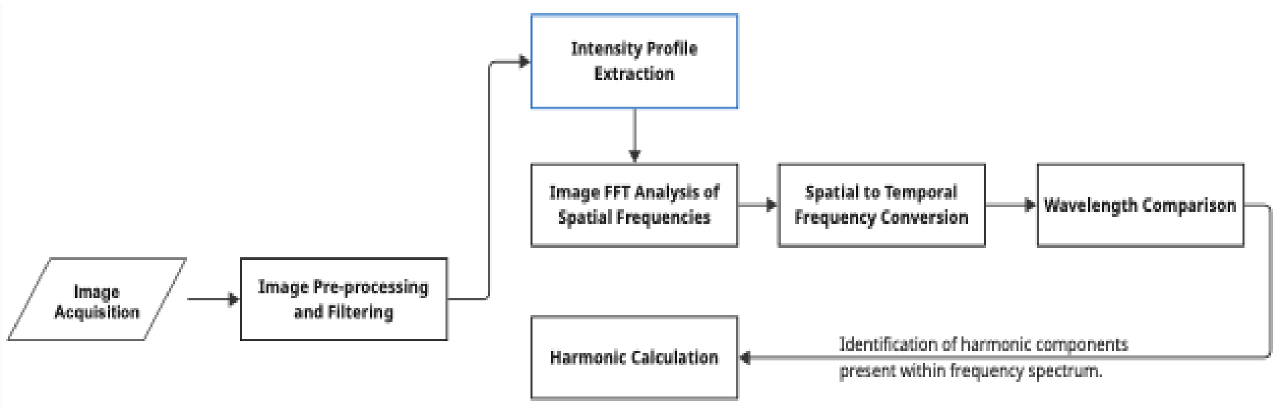

Fig. 1. Schematic diagram of methodology for machined surface image analysis

To ensure a robust image analysis method, all initial image acquisition was deliberately conducted outside the machine tool chamber. This crucial decision, coupled with an external light ring for consistent illumination, aimed to mitigate inherent challenges of in-situ imaging and prevent potential negative effects from early image processing steps. Developing a robust image analysis methodology involves a systematic and iterative testing framework. The acquired images were then processed in MATLAB, with a central focus on extracting key features indicative of machining quality and dynamics. A primary analytical step involved extracting intensity profiles from specific regions of interest within the images. This rich spatial information was then subjected to Fast Fourier Transform (FFT) analysis, both spatially and temporally.

The spatial FFT yielded dominant spatial wavelengths, which were critically compared with the theoretical feed per revolution. This comparison served as a robust validation point, as discrepancies could indicate issues like tool wear, material irregularities, or machine vibration effects impacting the desired surface finish. Similarly, the temporal FFT of the image data, derived from sequences of frames or specific time-series data extracted from the images, allowed to identify inferred temporal frequencies. Within these temporal frequency spectra, the attention was specifically directed towards identifying harmonics. The presence and amplitude of these harmonics provide robust indicators of periodic phenomena within the machining process, potentially pointing to chatter, imbalances, or specific operational frequencies, all of which are crucial for maintaining process stability and part quality.

By performing these analyses on clean, high-fidelity images, and focusing on fundamental physical relationships (like feed per revolution) and characteristic frequency signatures (harmonics), this approach significantly enhanced the robustness and reliability of the insights derived, making the methodology less susceptible to the typical noise and variability of an industrial environment.

3. RESULTS

3.1. MACHINING AND SURFACE ANALYSIS

Machining of slots based on the provided in Table 1 parameters. The main consideration of this test was to acquire different surface texture, which contains error transmitted machining system, such as vibrations. More information about machining test can be read in the paper [15]. The surfaces were captured by using designed on-machine surface measurement (OMSM) system. As a baseline, surfaces were measured using Zygo Nview7300 White Light Interferometer (WLI), with 10 times magnification and 1MPx CCD camera. The spacing of the 3D surface data was 1.09 µm × 1.09 µm × 0.0087 nm. The surface data are presented in Table 3.

Interestingly, standard parametric analyses of these WLI-measured surfaces did not reveal substantial differences, suggesting a deceptive similarity at a macroscopic level. However, a more granular examination of the extracted surface profiles clearly exposed distinct variations in characteristic features. These differences manifested as subtle yet undeniable profile irregularities, which can hypothesize are direct consequences of either the inherent dynamics of the machining system or specific nuances within the machining process itself. This observation underscores the value of detailed profile scrutiny, even when conventional roughness parameters appear consistent.

Table 3. Surface data measured using WLI, machined with 2 mm depth of cut

Image from slot 1	Image from slot 6	Image from slot 12
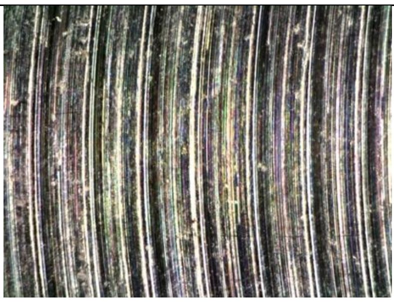	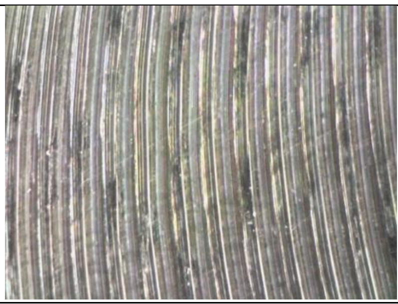	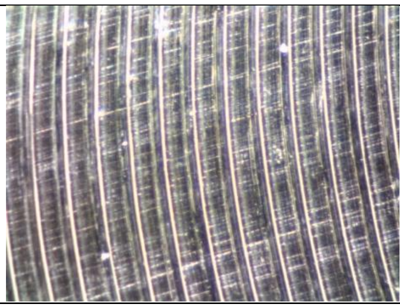
Surface texture analysis from WLI microscope		
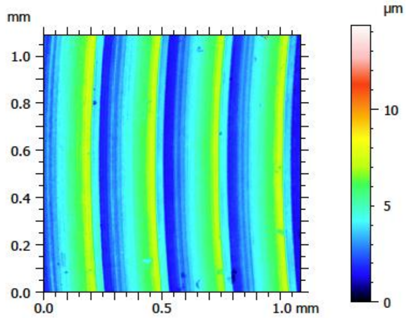	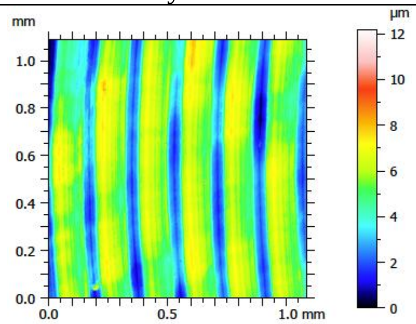	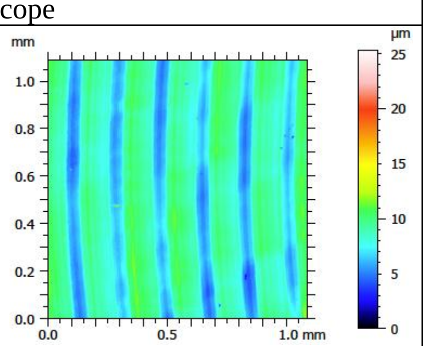
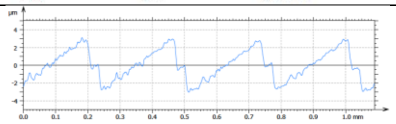	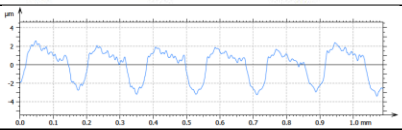	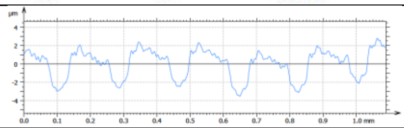

Slot 1:

Information	
Filter settings	Double Gaussian filter, 0.008 mm.

Parameters	Value	Unit
Rk	0.0877	µm
Rpk	0.0523	µm
Rvk	0.0638	µm
Mr1	11.5	%
Mr2	82.7	%
A1	3.01	µm²/mm
A2	5.51	µm²/mm
Rpk*	0.0896	µm
Rvk*	0.146	µm

Slot 6:

Information	
Filter settings	Double Gaussian filter, 0.008 mm.

Parameters	Value	Unit
Rk	0.115	µm
Rpk	0.0442	µm
Rvk	0.0505	µm
Mr1	7.42	%
Mr2	88.8	%
A1	1.64	µm²/mm
A2	2.84	µm²/mm
Rpk*	0.0976	µm
Rvk*	0.110	µm

Slot 12:

Information	
Filter settings	Double Gaussian filter, 0.008 mm.

Parameters	Value	Unit
Rk	0.107	µm
Rpk	0.0345	µm
Rvk	0.063	µm
Mr1	6.20	%
Mr2	85.5	%
A1	1.07	µm²/mm
A2	4.58	µm²/mm
Rpk*	0.0643	µm
Rvk*	0.111	µm

3.2. MACHINED SURFACE INTENSITY PROFILE ANALYSIS

This section details the methodology and immediate findings from the quantitative assessment of machined surface characteristics, leveraging detailed intensity profiles derived from acquired images. This granular analysis provides critical insights into the underlying machining process and system dynamics, aiming to reveal features not apparent through conventional macroscopic examinations. To ensure the robustness and reliability of the intensity data, free from typical industrial disturbances, all images were captured deliberately outside the machine tool chamber. This acquisition strategy employed an external light ring to provide uniform and consistent illumination across the workpiece surfaces. The resultant high-fidelity images formed the foundation for all subsequent analyses.

The acquired images, specifically those depicting machined surfaces, were then processed. Image files were loaded, converted to grayscale, and pre-processed with a median filter to reduce noise. Intensity profiles were then systematically extracted along a representative horizontal line (Fig. 2a, Fig. 3a), transforming the two-dimensional image data into one-dimensional intensity variations that reflect surface topography.

Following intensity profile extraction, a Fast Fourier Transform (FFT) was applied to these spatial profiles to transition the data from the spatial domain to the frequency domain. This transformation allowed for the identification of dominant spatial wavelengths present on the machined surfaces. The single-sided amplitude spectrum was derived from the absolute values of the FFT results, and leading spatial frequencies were identified. For both the "odd slot" and "even slot" surfaces, the dominant spatial wavelength identified from the FFT spectrum was then compared with the theoretical feed per revolution of the machining process.

Peaks in the frequency spectrum correspond to the dominant spatial frequencies present on the surface. The location of these peaks indicates the wavelength of periodic patterns (like feed marks or vibration-induced waves), and their amplitude reflects the prominence of these patterns. Machine tool vibrations, especially forced vibrations and chatter, leave characteristic periodic patterns on the machined surface.

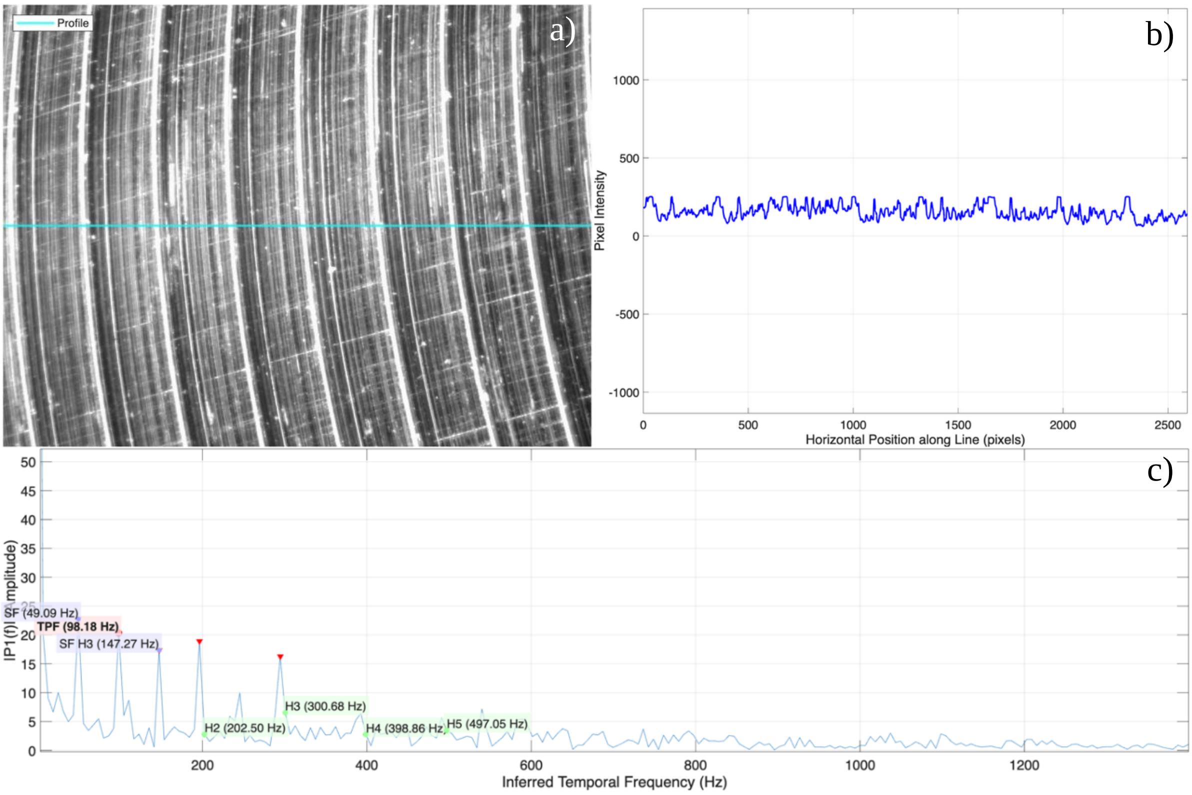

Fig. 2. a) Grayscale image with horizontal line representing profile extraction position, b) extracted intensity profile, c) an example of the Inferred Temporal Frequency Spectrum (from Spatial FFT) of even slot (slot 17), with first five (5) harmonics for Spindle Speed Frequency (SF) and Tooth Passing Frequency (TPF)

For the "odd slot" samples, with machining parameters of 3000 RPM and 540 mm/min feed, the theoretical feed per revolution was 0.1800 mm/revolution. The image analysis yielded a dominant spatial wavelength of 0.1833 mm, corresponding to a dominant spatial frequency of 5.4545 cycles/mm. This showed agreement, with a difference of only 1.85% from the theoretical value. Similarly, for the "even slot" surfaces, machined with 4000 RPM and 720 mm/min feed, the theoretical feed per revolution was also 0.1800 mm/revolution. The dominant spatial wavelength from the “even slot” image analysis was also 0.1833 mm (5.4545 cycles/mm), similarly demonstrating good agreement with the theoretical value (1.85% difference). This consistent alignment for both slot types suggests that the primary tool mark wavelength on the surface is robustly captured and aligns well with the expected kinematic imprint of the tool's feed.

In parallel, temporal information was inferred by converting the spatial frequencies into temporal frequencies using the theoretical feed rate. A FFT was subsequently applied to these inferred temporal frequencies to identify periodic phenomena within the machining process (Fig. 2c, Fig. 3c). A key objective of this temporal analysis was to specifically look for the presence and characteristics of harmonics within the frequency spectra, particularly those related to the Theoretical Spindle Speed Frequency (SF) and Theoretical Tooth Passing Frequency (TPF).

For the “odd slot” samples, the theoretical SF was 50.00 Hz and the TPF was 100.00 Hz. The temporal FFT spectra revealed the fundamental TPF at 98.18 Hz with an amplitude of 20.36, showing good agreement with the expected value. Furthermore, distinct higher-order TPF harmonics were identified, including Harmonic 2 (at 202.50 Hz, expected 200.00 Hz), Harmonic 3 (at 300.68 Hz, expected 300.00 Hz), Harmonic 4 (at 398.86 Hz, expected 400.00 Hz), and Harmonic 5 (at 497.05 Hz, expected 500.00 Hz). The fundamental SF was also found at 49.09 Hz (expected 50.00 Hz) with a dominant amplitude of 22.75, and its third harmonic (SF H3) was also present. This pattern indicates a stable machining process for the “odd slot” configuration, with the expected kinematic frequencies prominently represented.

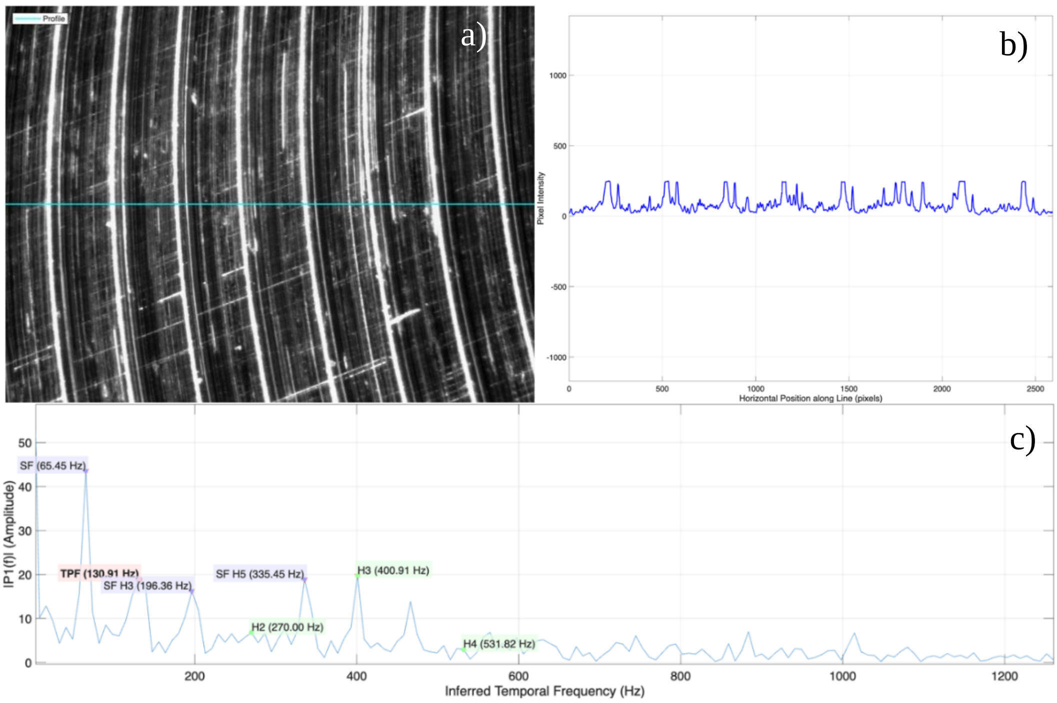

Fig. 3. a) Grayscale image with horizontal line representing profile extraction position, b) extracted intensity profile, c) an example of the Inferred Temporal Frequency Spectrum (from Spatial FFT) of even slot (slot 34), with first five (5) harmonics for Spindle Speed Frequency (SF) and Tooth Passing Frequency (TPF)

In contrast, the “even slot” samples, with a theoretical SF of 66.67 Hz and TPF of 133.33 Hz, exhibited a different temporal frequency signature. The fundamental TPF was found at 130.91 Hz with an amplitude of 18.91. Notably, the third TPF harmonic (TPF H3) at 400.91 Hz (expected 400.00 Hz) showed a relatively high amplitude of 19.72, nearly matching that of the fundamental TPF. The fundamental SF itself was highly prominent, found at 65.45 Hz (expected 66.67 Hz) with a significantly larger amplitude of 43.50, almost double that of its TPF counterpart. The third (SF H3) and fifth (SF H5) SF harmonics were also clearly detected. The presence of these higher-amplitude SF components and specific TPF harmonics for the “even slot” suggests a more pronounced influence of spindle-related dynamics or specific resonant conditions (including vibrations) during this machining configuration, which warrants further investigation into its impact on surface integrity and process stability.

These comprehensive spatial and temporal FFT analyses of machined surface intensity profiles allowed for a detailed, quantitative characterization of surface features that might be overlooked by macroscopic or conventional parametric assessments.

4. DESIGN OF ON MACHINE SURFACE MEASUREMENT SYSTEM

While many studies have been conducted to explore the on-machine implementation of the non-contact 3D surface measurements of the workpiece via interferometry [1, 17], deflectrometry [18], confocal microscopy [13, 19] and autostereoscopic [20] systems for measuring workpiece profile error and tool wear, use of machine vision systems integrated to machining centers for acquiring surface characteristics is not well explored. Especially, robust machine vision systems which can withstand the environment inside the machining chamber is not proposed. An embedded camera assembly with an actuated cover is developed for this study to meet the following requirements ease of integration to existing machining tool, ease of customization and duplication for allow different camera/lighting configurations, and sufficient protection against cutting chips and fluids

The assembly consists of three stationary parts (marked blue in Fig. 4) and one actuated part (marked red in Fig. 4), all of which fabricated with commercial FDM printer. The printed parts are made of ABS plastic to account for higher operational temperatures and vibration.

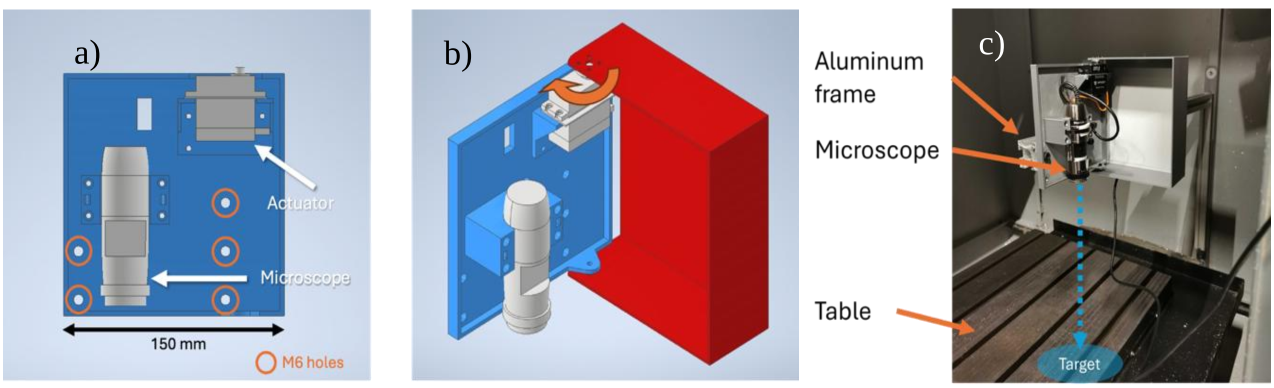

Fig. 4. OMSM assembly, a) Front view without the cover, b) Projection view with the actuated cover, c) OMSM assembly in machining chamber, example

The use of multiple parts instead of monolithic design allows easier adjustment of the camera alignment around X and Y-axes, as well as replacing machine vision system without remaking the entire assembly. The actuated cover can be closed while machining to prevent the damages to the camera due to cutting chips and coolant and be opened when the workpiece imaging is to be conducted (Fig. 4b). The design also features five M6 holes (marked orange circles in Fig. 4a), which allows the assembly to be installed either directly to the spindle housing, or with an aluminum profile to any interior surface (Fig. 4c).

The illumination pattern was enhanced through the integration of a coaxially mounted light ring in conjunction with the DinoLite camera.

5. CONCLUSION

This study demonstrates the feasibility of using a CCD camera mounted inside the machining chamber to capture images containing sufficient data to correlate the generated surface with the machining process. This approach can enhance machine productivity. The method shows potential to complement existing analysis techniques by reducing the time required for analysis and feedback regarding unwanted vibrations in the machining system.

The experiment underscores the critical importance of capturing images with sufficiently high quality to enable the extraction of essential data. Illumination presents a significant challenge due to the reflective properties of the workpiece. The DinoLite camera has inbuilt lightning. However, the designed proved to not give sufficiently uniformed light and had to be completed by an external device. The adopted strategy to mitigate this involved uniformly flooding the object with light from directly above, centred around the camera. Ensuring uniform lighting is crucial, as local variations in light intensity introduce noise and degrade the fidelity of the data acquired by the CCD sensor.

Image-based spatial frequency analysis consistently validates theoretical feed per revolution. For both “odd slot” and “even slot” machined surfaces, the dominant spatial wavelength extracted from image intensity profiles through FFT analysis showed excellent agreement (within 1.85% difference) with the theoretical feed per revolution. This indicates that the image analysis method robustly captures the primary kinematic imprints on the machined surface, confirming the expected tool mark wavelength regardless of specific machining parameters used for each slot type.

Temporal harmonic analysis reveals distinct machining process dynamics for different slot types. While spatial characteristics were consistent, the temporal FFT spectra showed notable differences between the “odd slot” and “even slot” surfaces. The “odd slot” exhibited a stable process with expected fundamental and higher-order Tooth Passing Frequency (TPF) harmonics. In contrast, the “even slot” displayed a more pronounced influence of Spindle Speed Frequency (SF) components and specific TPF harmonics, suggesting potentially different spindle-related dynamics or resonant conditions impacting the surface during its machining. The clear distinctions observed between the “odd slot” and “even slot” characteristics, particularly in terms of dominant spatial wavelength alignment and the specific patterns and amplitudes of temporal harmonics, provide robust, frequency-domain signatures directly informing the understanding of the machining system's performance and process integrity.

FFT analysis of surface images can reveal the frequencies of patterns, which can be directly correlated to the vibration frequencies of machine tool components (e.g., spindle imbalance, structural resonances).

The image analysis approach, encompassing both spatial and temporal Fast Fourier Transform (FFT) of intensity profiles, proves to be a highly effective and robust methodology for characterizing machined surfaces. It not only consistently validates theoretical kinematic parameters, such as the feed per revolution, by precisely identifying the dominant spatial wavelength of tool marks, but also critically reveals subtle yet significant dynamic differences within the machining process through its detailed harmonic analysis. This capability to uncover frequency-domain signatures provides invaluable insights into machining system performance and process stability that might otherwise be overlooked by conventional macroscopic or parametric surface assessments.

6. FUTURE WORK

The next step in advancing this research is to comprehensively refine and further evaluate the parameters for image acquisition. This includes exploring various camera settings (e.g., exposure time, aperture, focal length), alternative illumination strategies (e.g., structured light, dark field illumination, coaxial lighting), and advanced optical setups to optimize the capture of specific surface features. Concurrently, a rigorous assessment of various image processing techniques is underway. The overarching goal is to ensure that the raw image data, and subsequent processed data, sufficiently highlight and accurately represent the desired characteristics of the surface, such as tool marks, chatter patterns, or material defects, which are crucial for process diagnostics.

Furthermore, a significant avenue of ongoing research involves leveraging the power of machine learning (ML), deep learning (DL), and transfer learning (TL) models. The aim is to train these advanced computational models to autonomously process and establish robust links between the detailed surface characteristics extracted from images and the underlying machining process parameters and conditions. This includes developing models capable of predicting surface roughness from image features, identifying the root cause of specific surface irregularities based on spectral signatures, and ultimately enabling real-time process monitoring and control through image-based feedback. Such data-driven approaches are essential for moving towards intelligent manufacturing systems capable of optimizing machining processes for desired surface quality and predicting potential anomalies [21, 22].

REFERENCES

[1] BUI L.V., MAC T.B., NGUYEN D.T., 2023, *Surface Roughness Investigation Through Interplay of Cutting Speed and Thermal-Assisted Machining in High-Speed Machining of Skd11 Steel*, Journal of Machine Engineering, 23/4, 33–42, https://doi.org/10.36897/jme/170980.

[2] ARCHENTI A., 2011, *A Computational Framework for Control of Machining System Capability from Formulation to Implementation*, Doctoral Thesis KTH Royal Institute of Technology, Department of Production Engineering, Machine and Process Technology, Stockholm, Sweden.

[3] LIU Y.P., ALTINTAS Y., 2021, *In-Process Identification of Machine Tool Dynamics*, CIRP J. Manuf. Sci. Technol., 32, 322–337, https://doi.org/10.1016/j.cirpj.2021.01.007.

[4] KIZAKI T., TSUJIMURA S., MARUKAWA Y., MORIMOTO S., KOBAYASHI H., 2021, *Robust and Accurate Prediction of Thermal Error of Machining Centers Under Operations with Cutting Fluid Supply*, CIRP Annals, 70/1, 325–328, https://doi.org/10.1016/j.cirp.2021.04.074.

[5] TANAKA S., KIZAKI T., TOMITA K., TSUJIMURA S., KOBAYASHI H., SUGITA N., 2022, *Robust Thermal Error Estimation for Machine Tools Based on In-Process Multi-Point Temperature Measurement of a Single Axis Actuated by a Ball Screw Feed Drive System*, J. Manuf. Process., 85, 262–271, https://doi.org/10.1016/j.jmapro.2022.11.037.

[6] BRYAN J.B., 1982, *A Simple Method for Testing Measuring Machines and Machine Tools Part 1, Principles and Applications.* Precision Engineering 4/2, 61–69, https://doi.org/10.1016/0141-6359(82)90018-6.

[7] BRYAN J.B., 2021, *A Simple Method for Testing Measuring Machines and Machine Tools Part 2: Construction Details*, Precision Engineering 4/3, 125–138, https://doi.org/10.1016/0141-6359(82)90075-7.

[8] IBARAKI S., OKUMURA R., 2021, *A Machining Test to Evaluate Thermal Influence on the Kinematics of a Five-Axis Machine Tool*, Int. J. Mach. Tools Manuf., 163, https://doi.org/10.1016/j.ijmachtools.2021.103702.

[9] *Standard – Test Conditions for Machining Centres – Part 10: Evaluation of Thermal Distortions ISO 10791-10:2022*, n.d. Svenska institutet för standarder, SIS, 2025. https://www.sis.se/produkter/produktionsteknik/industriell-processtyrning/fleroperationsmaskiner/ISO-10791-102022/.

[10] JAQUEMOD A., PALALIC M., GÜZEL K., MÖHRING H.C., 2024, *In-Process Monitoring of Inhomogeneous Material Characteristics Based on Machine Learning for Future Application in Additive Manufacturing*, Journal of Machine Engineering, 24/2, 83–93, https://doi.org/10.36897/jme/187872.

[11] QUINSAT Y., TOURNIER C., 2011, *In Situ Non-Contact Measurements of Surface Roughness*, Precis. Eng., 36/1, 97–103, https://doi.org/10.1016/j.precisioneng.2011.07.011.

[12] FU S., CHENG F., TJAHJOWIDODO T., ZHOU Y., BUTLER D., 2018, *A Non-Contact Measuring System for In-Situ Surface Characterization Based on Laser Confocal Microscopy*, Sensors (Switzerland), 18/8, https://doi.org/10.3390/s18082657.

[13] ZOU X., ZHAO X., LI G., LI Z., SUN T., 2017, *Non-Contact on-Machine Measurement Using a Chromatic Confocal Probe for an Ultra-Precision Turning Machine*, International Journal of Advanced Manufacturing Technology, 90/5-8, 2163–2172, https://doi.org/10.1007/s00170-016-9494-3.

[14] SAMTAS G., 2014, *Measurement and Evaluation of Surface Roughness Based on Optic System Using Image Processing and Artificial Neural Network*, International Journal of Advanced Manufacturing Technology, 73/1–4, 353–364, https://doi.org/10.1007/s00170-014-5828-1.

[15] COLL M., SUN P., GADHAM F., ARCHENTI A., 2025, *Evaluating Spindle Degradation and Machining Quality Using an Exchangeable Spindle Unit and Vibration-Based Monitoring*, euspen's 25th International Conference & Exhibition, Zaragoza, ES, June 2025 Spain.

[16] ZHANG C., ZHANG J., 2013, *On-Line Tool Wear Measurement for Ball-End Milling Cutter Based on Machine Vision*, Comput. Ind., 64/6, 708–719, https://doi.org/10.1016/j.compind.2013.03.010.

[17] LI D., TONG Z., JIANG X., BLUNT L., GAO F., 2018, *Calibration of an Interferometric on-Machine Probing System on an Ultra-Precision Turning Machine*, Measurement (Lond), 118, 96–104, https://doi.org/10.1016/j.measurement.2017.12.038.

[18] RÖTTINGER C., FABER C., KURZ M., OLESCH E., HÄUSLER G., UHLMANN E., *Deflectometry for Ultra-Precision Machining-Measuring without Rechucking*, [Online] Available: http://www.dgao-proceedings.de.

[19] Ye L., Qian J., Haitjema H., Reynaerts D., 2022, *On-Machine Chromatic Confocal Measurement for Micro-EDM Drilling and Milling*, Precis. Eng., 76, 110–123, https://doi.org/10.1016/j.precisioneng.2022.03.011.

[20] LI D., CHEUNG C.F., REN M., ZHOU L., ZHAO X., 2014, *Autostereoscopy-Based Three-Dimensional on-Machine Measuring System for Micro-Structured Surfaces*, Opt. Express., 22/21, 25635, https://doi.org/10.1364/oe.22.025635.

[21] WOLF J., BANDARU N.K., DIENWIEBEL M., MÖHRING H.C., 2025, *Image Based Detection of Coating Wear on Cutting Tools with Machine Learning*, Journal of Machine Engineering, 25/1, 57–67, https://doi.org/10.36897/jme/196725.

[22] GREITLER J.A., NOBEL N., BLEICHER F., 2025, *Wavelet Decomposition of Close-To-Process Acceleration Signals for Wear Monitoring*, Journal of Machine Engineering, 25/3, 18–26, 2025, https://doi.org/10.36897/jme/209759.